Electronic Supplementary Information (ESI) for

Nanofiller-tuned microporous polymer molecular sieves for energy and environmental processes

Qilei Song,[ab] Shuai Cao,[c] Robyn H. Pritchard,[a] Hazim Qiblawey,[d] Eugene M. Terentjev,[a] Anthony K. Cheetham [c] and Easan Sivaniah[ae]**

[a] *Cavendish Laboratory, Department of Physics, University of Cambridge, Cambridge CB3 0HE, UK.*

[b] *Department of Chemical Engineering, Imperial College London, London SW7 2AZ, UK. Email: q.song@imperial.ac.uk*

[c] *Department of Materials Science & Metallurgy, University of Cambridge, Cambridge CB3 0FS, UK.*

[d] *Department of Chemical Engineering, College of Engineering, Qatar University, Qatar*

[e] *Institute for Integrated Cell-Material Sciences (iCeMS), Kyoto University, Kyoto 606-8501, Japan. Email: esivaniah@icems.kyoto-u.ac.jp*

Experimental methods

Synthesis of polymer. The PIM-1 polymer was synthesised following the method invented by Budd and McKeown[1], from polycondensation reaction of 5,5′,6,6′-tetrahydroxy-3,3,3′,3′-tetramethylspirobisindane (TTSBI, Alfa Aesar) and 2,3,5,6-tetrafluoroterephthalonitrile (TFTPN, Matrix Scientific) in the presence of K_2CO_3 (Aldrich) in anhydrous dimethylformamide. After the mixture has been stirred at 60 ℃ for about 48 h, the polymer was purified by dissolving in chloroform and re-precipitation from methanol, filtered and dried in vacuum oven at 110 ℃ for overnight. The molecular weight of purified polymer was determined from gel permeation chromatography (GPC), giving an average molecular weight of M_n= 80, 000 to 100,000 dalton and a polydispersity (PDI) of 2.0.

Preparation of films. Thick dense polymer films were prepared by solution casting of polymer solution in chloroform. Non-dissolved particles were removed by filtration through PTFE filters or by centrifugation. Polymer solutions were casted on clean glass substrate in a glove box. After the solvent has been slowly evaporated at room temperature in two days, the dry free-standing films were obtained and exposed to methanol soaking for overnight and dried in air. After, the films were dried in a vacuum oven at 120 ℃ for 24 h.

Fabrication of nanocomposite films. Nanocomposite films were prepared from the colloidal solution of polymer/nanoparticle mixture following our previous approach.[2] Two types of nanoparticles were used as fillers: (1) porous zeolitic imidazolate framework (ZIF-8) nanocrystals with diameter of 60-100 nm were synthesized by rapid reaction of zinc nitrate hexahydrate [$Zn(NO_3)_2$ $6H_2O$] and 2-methylimidazole ($C_4H_6N_2$) in methanol following Cravillon *et al.*[3], (2) nonporous inorganic silica nanoparticles (aggregation size of 200-300 nm) with an average primary particle size of 12 nm (99.8% trace metals basis, Sigma Aldrich). The nanoparticles were dispersed in chloroform and then mixed with PIM-1 polymer solution and thoroughly stirred for two days. After, the mixture was bubbled with pure N_2 to slowly evaporate excess solvent, and then the homogeneous and viscous solutions were casted to form nanocomposite films, following the same protocol of solution casting and post treatment as pure polymer films.

Thermal treatment. The polymer films were exposed to thermal treatment under controlled atmosphere in a high-temperature vacuum oven (Heraeus, 20-400 ℃). The vacuum oven was modified allowing operation in

controlled vacuum or purging mode. The pressure was monitored continuously by pressure transmitters (Keller Ltd, UK). A series of experiments were performed by heating the polymer films at different temperature under continuous controlled vacuum (1 mbar). Flat polymer films were placed on the plate in the vacuum oven and heated under vacuum at 120 ℃ for 3 h, then heated to final temperature at 10 ℃ min^{-1}. Then the samples were maintained at the temperature for extended time up to 24 h. Thermal-oxidative crosslinking (degradation) of polymer films were also performed in a thermogravimetric analyser (TGA) in well-controlled atmosphere. A batch of dense polymer films (~5 mg, dimension of 3×3 mm) were heated at 120 ℃ for 1 h under continuous flow of purging gas to remove moisture and residual gases, then heated at 10 ℃ min^{-1} to varied temperature (up to 385 ℃), then kept at 385 ℃ for 2 h. Throughout, the purge gas was certified O_2/Argon mixture (200 ppm O_2, balance argon, BOC).

Characterization methods. Scanning electron microscopy (SEM) was performed using a Hitachi S5500 microscope. The polymer films were fractured in liquid nitrogen and coated with a thin layer of gold (2-3 nm). Gel permeation chromatography (GPC) calibrated with polystyrene standards was used to quantify the molecular weight. The crosslinked polymer films were soaked in chloroform with weight fraction of insoluble gel quantified, while the molecular weight of soluble fraction was measured by GPC. FTIR analysis was carried out using the Bruker Tensor 27 Infrared Spectrometer, equiped with an attenuated total reflectance (ATR) cell. XRD patterns were collected with a Bruker D8 X-ray diffractometer operated at 40 mA and 40 kV using Cu Kα radiation with a step of 0.02 °/sec. X-ray photoemission spectra were measured *ex situ*, with an X-ray photoemission spectroscopy (ESCALAB 250Xi, Optoelectronics group, Cavendish Laboratory). The polymer films were evacuated under vacuum of 10^{-10} mbar for one hour prior to moving to the chamber for measurement. High-resolution spectra of O1s, C1s, and N1s were acquired first prior to survey spectra. The C-C peak at 284.8 eV was used as a charge correction reference. Tensile tests of polymer films were carried out at a home-made stretcher machine. The films (length of ~20 mm and width of ~2 mm) were stretched for 0.02 mm in each step with a relaxation time of 30 s, giving an apparent strain rate of ~4×10^{-5} s^{-1}. The average value of Young's modulus, the tensile strength at break and elongation at break were measured. Nanoindentation of polymer films were performed at ambient temperature using a sharp Berkovich tip in the continuous stiffness measurement (CSM) mode on an MTS NanoIndenter® XP (MTS Corp., Eden Prairie, MN). The indenter axes were aligned normal to the membrane planes. The average values of the Young's modulus (*E*) and the hardness (*H*) were extracted from the force-displacement *P-h* curves over depths of 100–1000 nm, with a series of 20 measurements at different locations.

Gas sorption. Low-pressure gas sorption was performed with Micromeritics ASAP 2020 with pressure up to 1 bar. Dense polymer films (~0.1 g) with thickness of ~50 μm were cut into small pieces and degassed at 120 ℃ under high vacuum(<10^{-6} bar) prior to the gas sorption measurement. Nitrogen adsorption-desorption isotherms were measured at 77 K. Gas sorption isotherms of N_2, CO_2 and CH_4 were also measured at 273 K.

Gas permeation. Pure gas permeation was carried out using a constant volume apparatus following the time-lag method, with feed pressure at 4 bar and temperature of 22 ℃. Detailed information can be found in our recent study.[2] Mixed gas permeation was performed in another membrane permeation apparatus using constant flow method. The membrane was exposed to certified feed gas mixtures (BOC, UK) of CO_2/CH_4 (50/50 vol.%) and CO_2/N_2 (50/50 vol.%) with pressure up to 35 bar at room temperature (22 ℃), with a stage cut (ratio of flow rates of permeate to feed) less than 1 %. The gas compositions were analyzed by a gas chromatograph (GC-2014, Shimadzu).

Thermal conductivity. The thermal conductivity of samples was measured using a hot disk thermal constants analyzer, at 25 ℃ and atmospheric pressure. An encapsulated Ni-spiral sensor is sandwiched between two pieces of flat thick discs (thickness of 2 mm, diameter of 20 mm, solution-casted using the same solution for preparation of dense membranes). The output of power is 0.05 W and measurement time is 5 seconds. The final thermal conductivity was averaged from 4-6 measurements. Pure PIM-1 polymer, ZIF-8 pellet, and PIM-1/ZIF-8 nanocomposites were measured. ZIF-8 nanocrystals were dried at 120 ℃ under vacuum and pelletized.

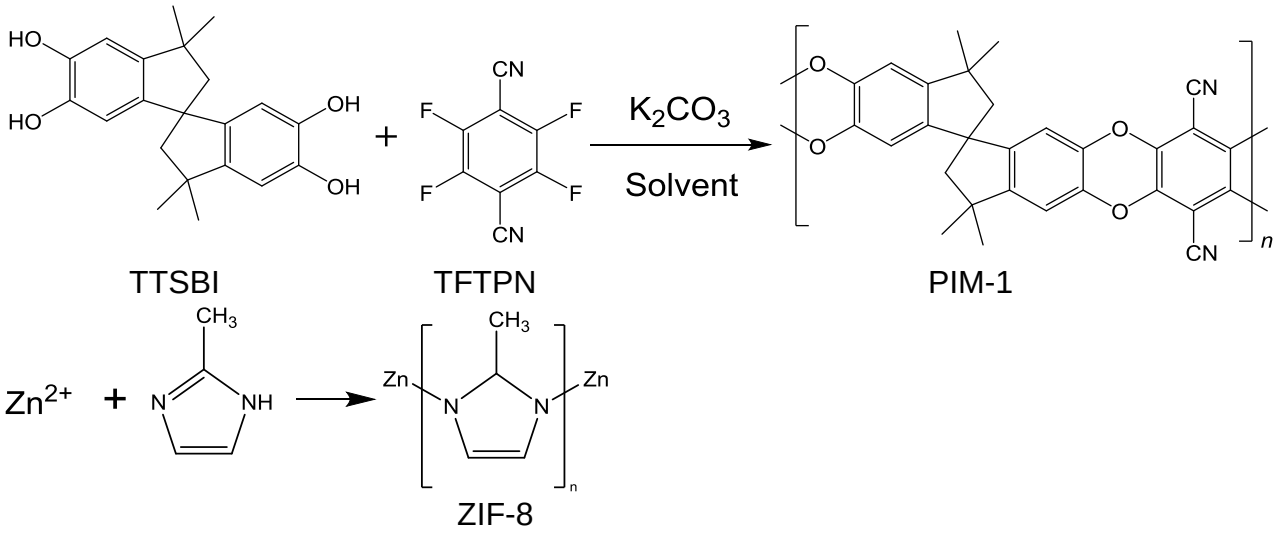

Fig. S1. Synthesis of PIM-1 polymer and ZIF-8. TTSBI: 5,5′,6,6′-tetrahydroxy-3,3,3′,3′-tetramethylspirobisindane; TTFPN: 2,3,5,6-tetrafluoroterephthalonitrile; Solvent was dimethylformamide. ZIF-8 nanocrystals were synthesized by rapid reaction of zinc nitrate hexahydrate [$Zn(NO_3)_2 \cdot 6H_2O$, Alfa Aesar] and 2-methylimidazole [$C_4H_6N_2$, Sigma-Aldrich] in methanol following Cravillon et al.[3] The detailed procedure of washing and processing can be found in our previous study.[2]

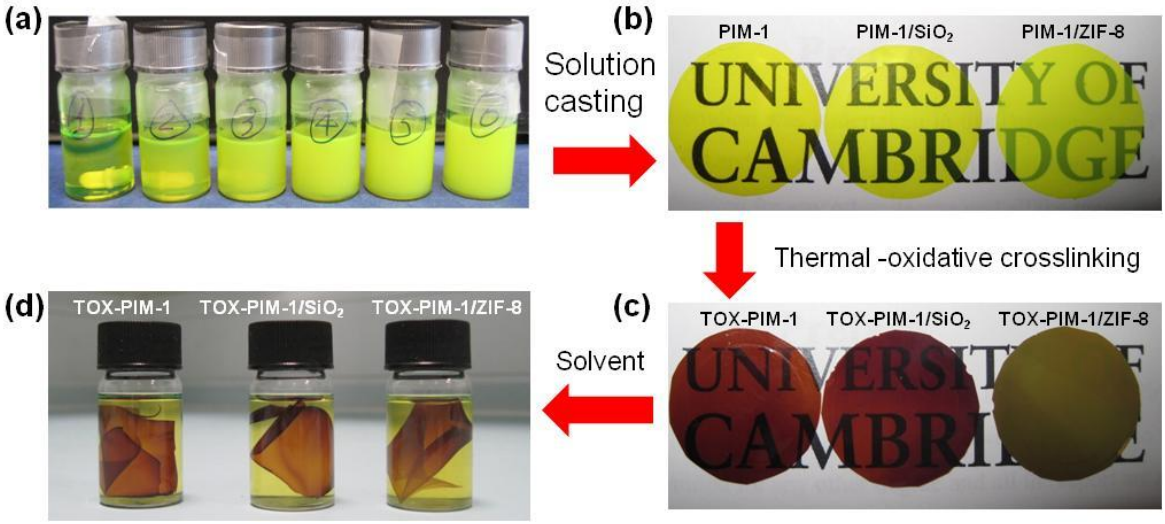

Fig. S2. Photos of polymer films. (a) Polymer solution and mixture of polymer and nanoparticles. (b) PIM-1 and nanocomposite films after solvent being evaporated and further exposure to annealing at 120 ℃ for 24 h. (c) Films after thermal oxidative crosslinking treatment, and (d) films became insoluble in chloroform solvent. TOX-PIM-1, TOX-PIM-1/SiO_2 and TOX-PIM-1/ZIF-8 were prepared by thermal oxidation at 385 ℃ for 24 h under vacuum (1 mbar). Loadings of SiO_2 nanoparticles and ZIF-8 nanocrystals in composite membranes are 20 wt%.

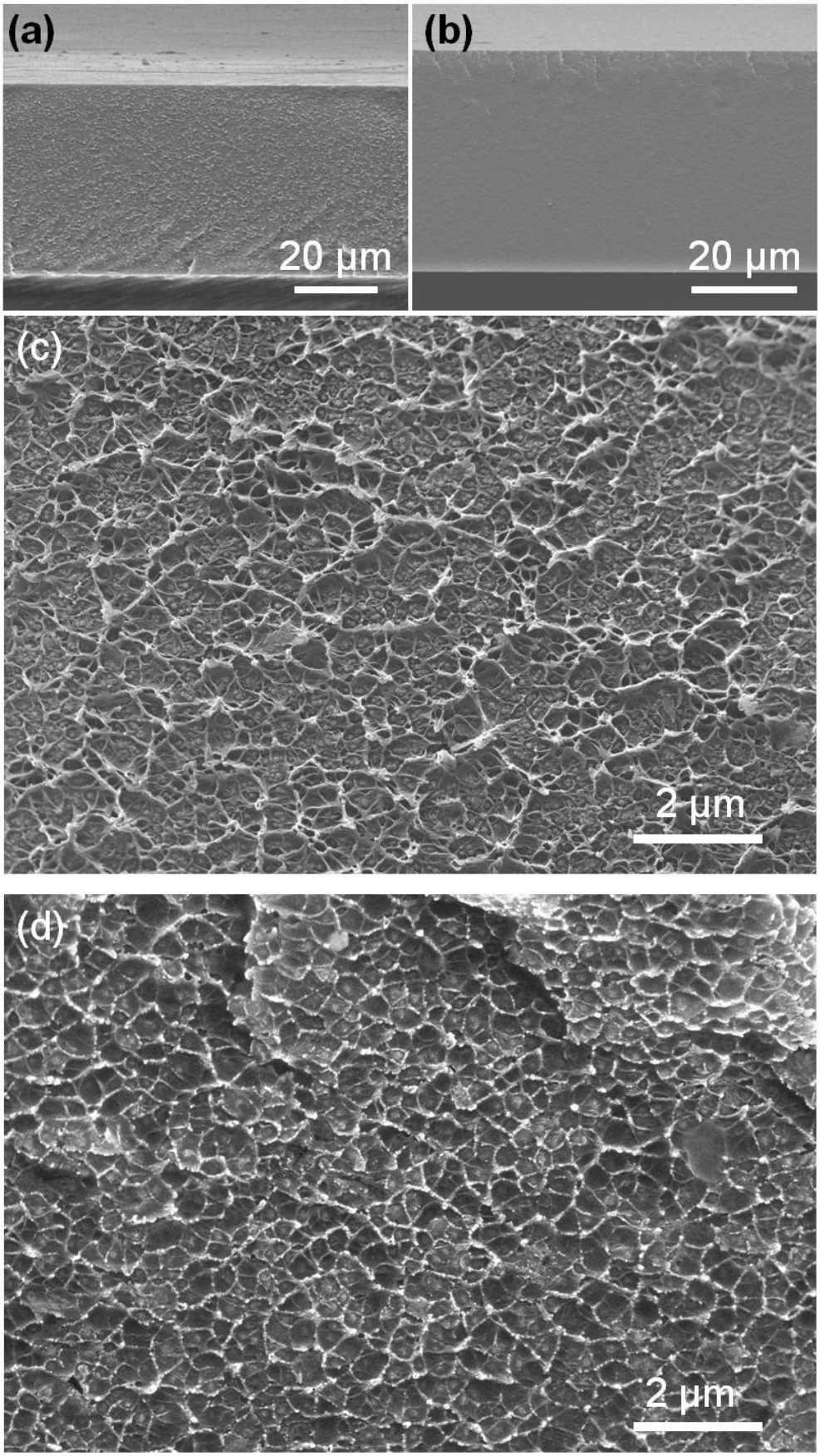

Fig. S3. Cross-sectional SEM images. (a, c) PIM-1/ZIF-8 (20 wt%), (b) PIM-1/nanosilica (20 wt%), and (d) thermal-oxidatively crosslinked PIM-1/ZIF-8 nanocomposite films (20 wt%), without observable microscopic voids.

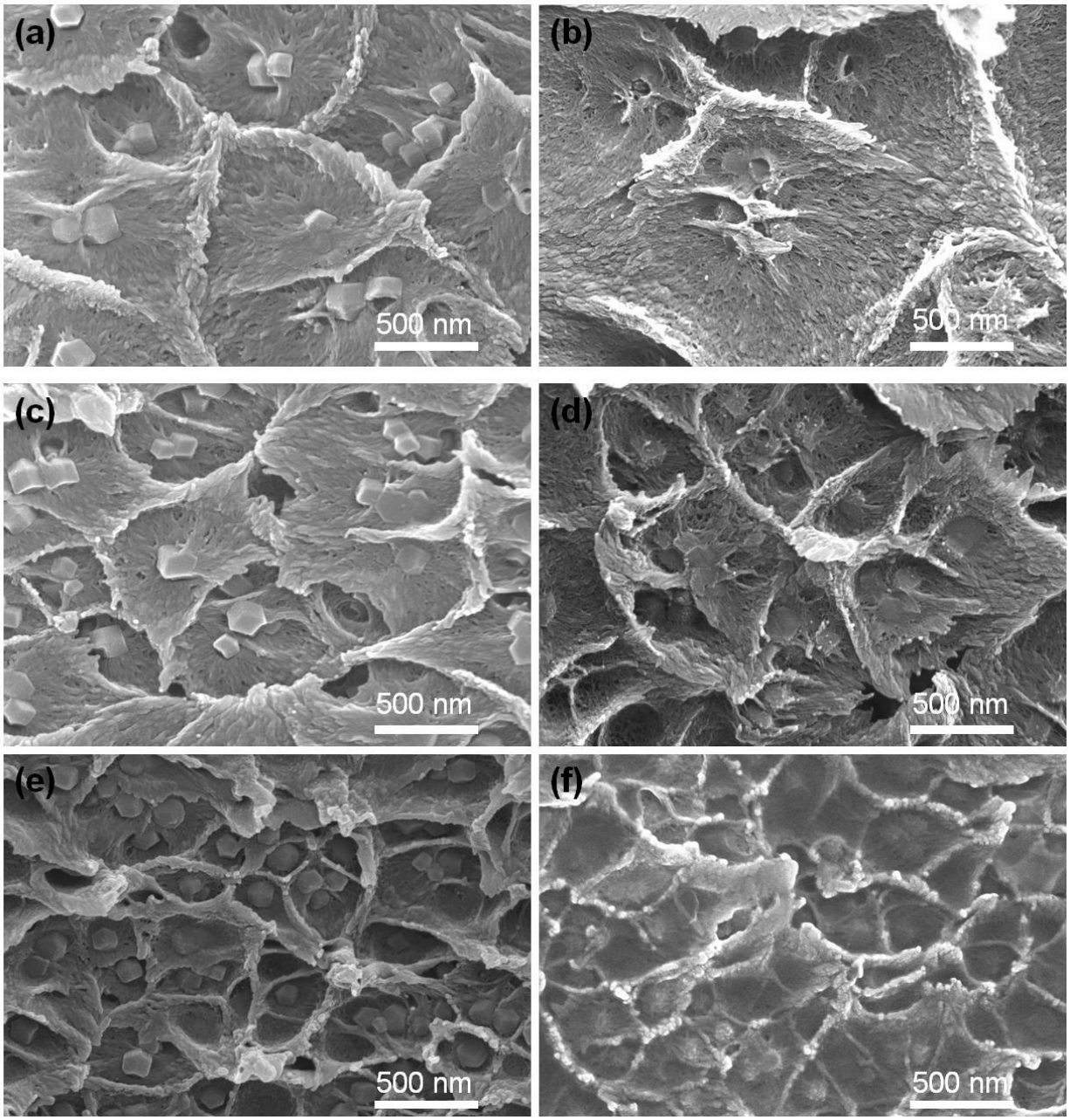

Fig. S4. Cross-sectional SEM images of PIM-1 polymer films incorporated with ZIF-8 nanocrystals. (a-b) 5wt%, (c-d) 10wt%, (e-f) 20wt%. (a, c, e) PIM-1/ZIF-8, (b, d, f) TOX-PIM-1/ZIF-8. The thermal oxidative crosslinking was performed by curing the polymer composite films at 385 ℃ for 24 h under vacuum (1 mbar).

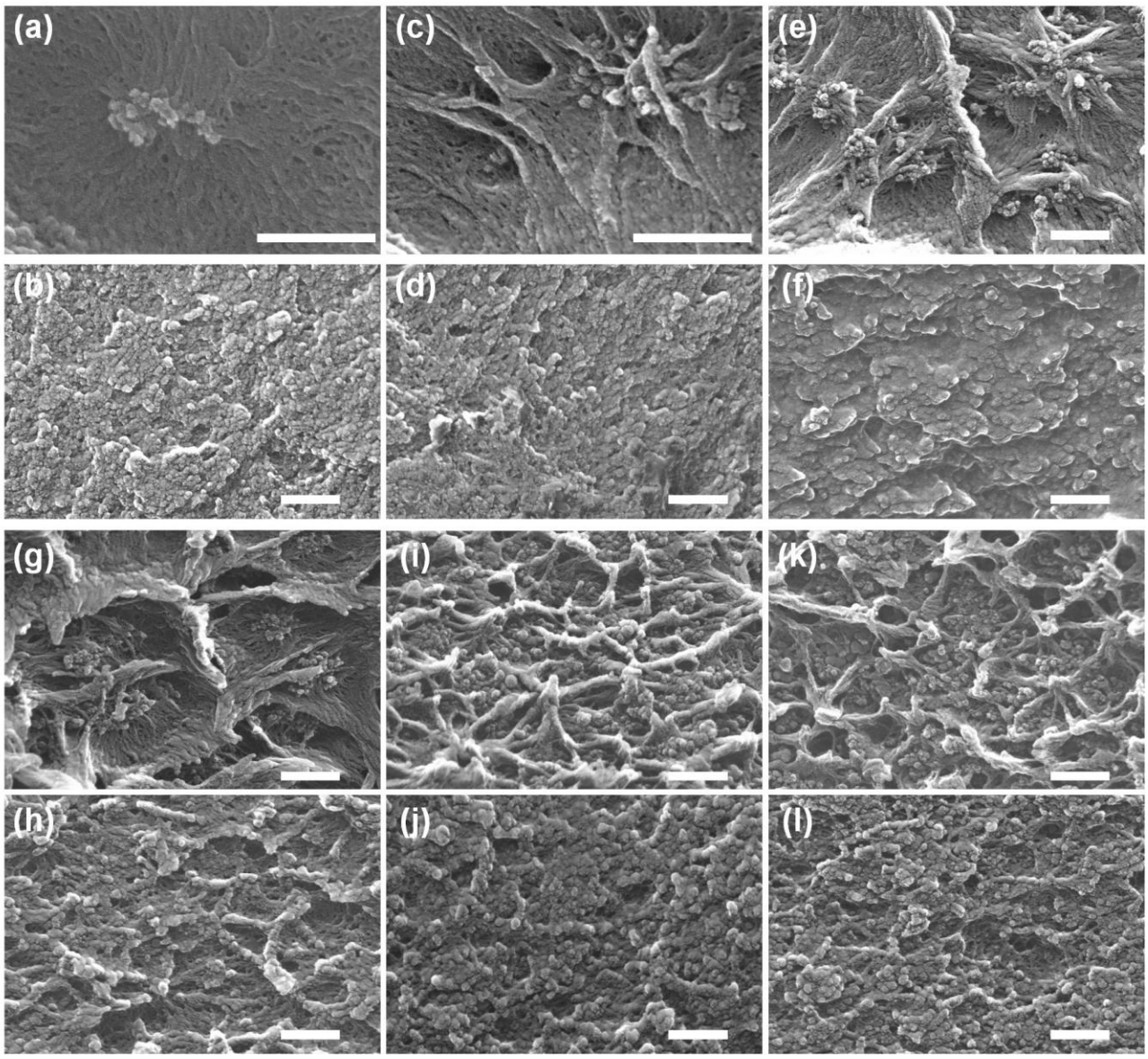

Fig. S5. SEM images of cross-sections of PIM-1/SiO_2 and TOX-PIM-1/SiO_2 nanocomposite films. (a-b) 1wt%, (c-d) 2wt%, (e-f) 5wt%, (g-h) 10 wt%, (i-j) 20wt%, (k-l) 30wt%. (a, c, e, g, i, k) PIM-1/SiO_2 annealed at 120 ℃ for 24 h. (b, d, f, h, j, l) TOX-PIM-1/SiO_2 composites, thermal-oxidatively crosslinked at 385 ℃ for 24 h under vacuum (1 mbar). Scale bar in all panels: 200 nm.

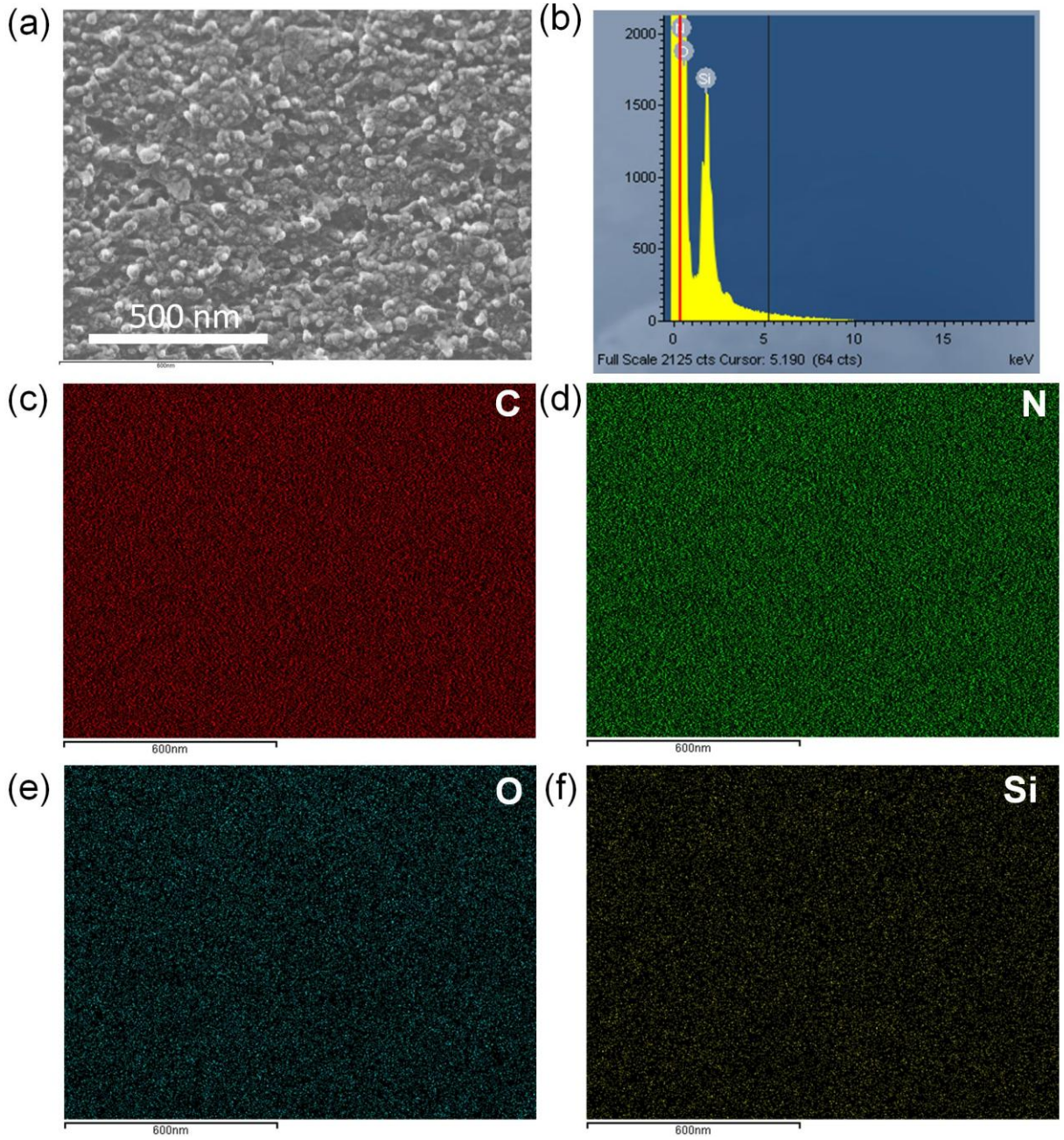

Fig. S6. SEM-EDX of cross-section of TOX-PIM-1/SiO2 nanocomposite films. (a) SEM, (b) EDX spectra, and element mapping of (c) carbon, (d) nitrogen, (e) oxygen, and (f) silicon.

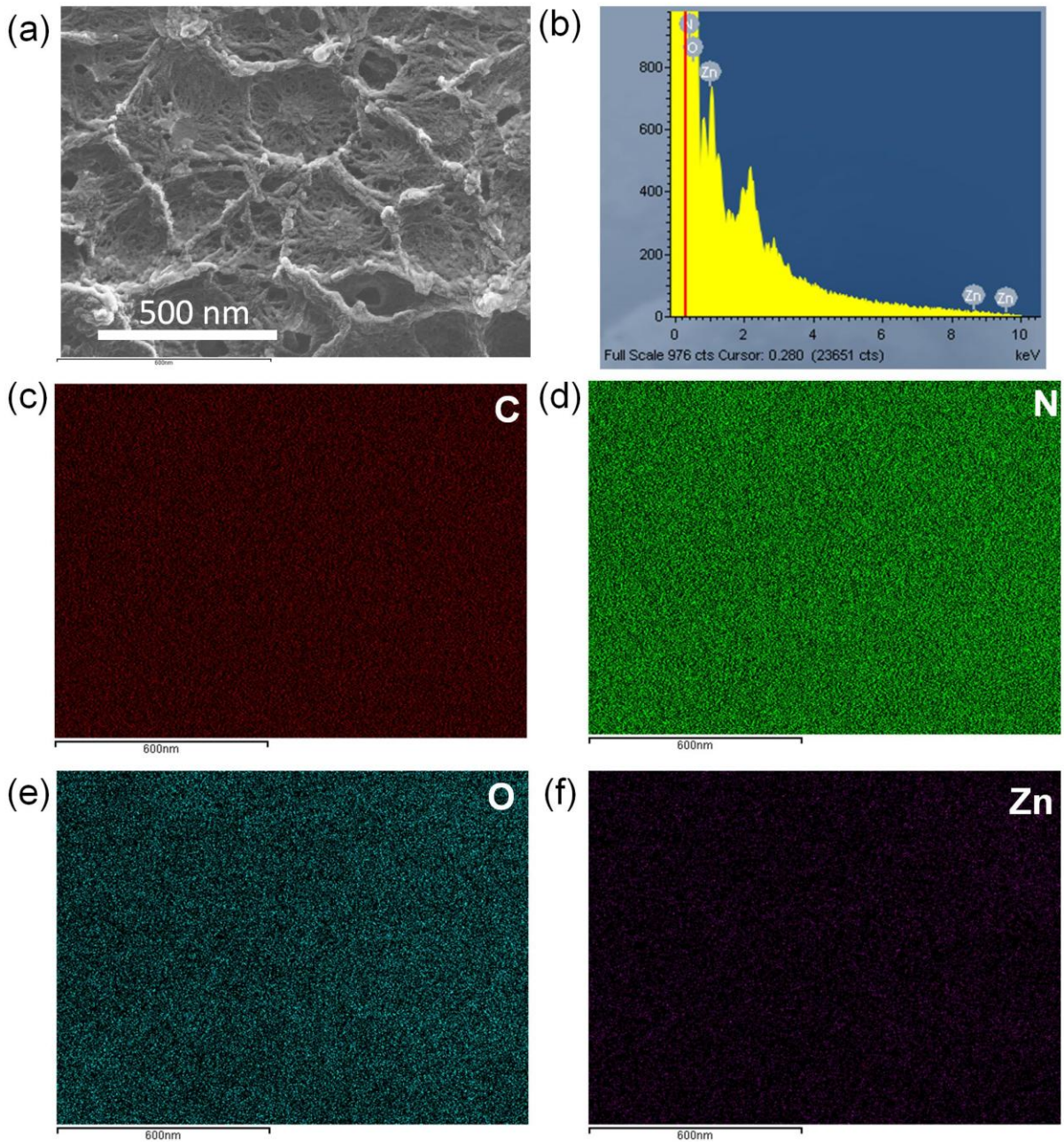

Fig. S7. SEM-EDX of cross-section of TOX-PIM-1/ZIF-8 nanocomposite films. (a) SEM, (b) EDX spectra, and element mapping of (c) carbon, (d) nitrogen, (e) oxygen, and (f) zinc.

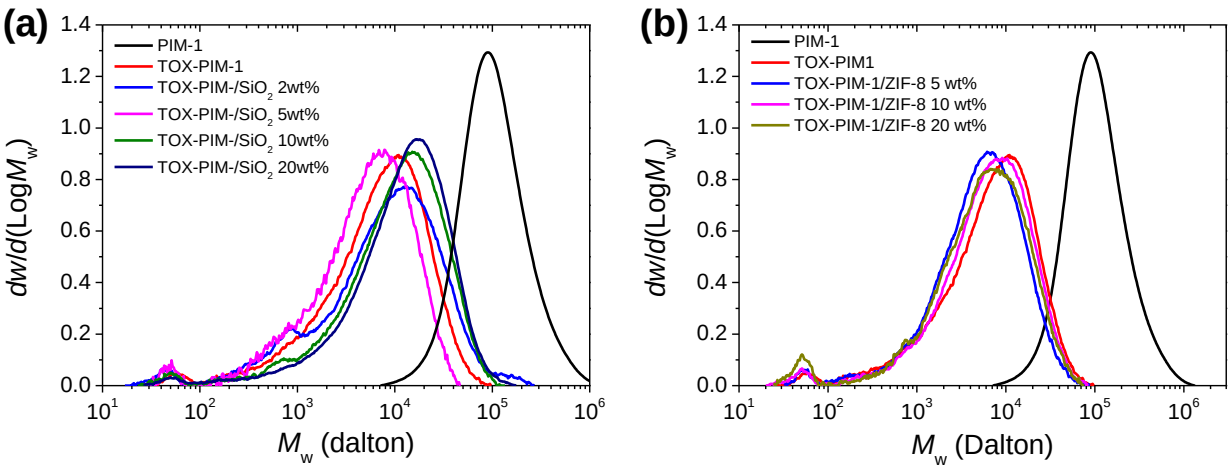

Fig. S8. Molecular weight distribution. The composite films after thermal oxidative crosslinking at 385 ℃ for 24 h was dissolved in chloroform and the soluble fraction was measured in GPC. The weight percentage of soluble fraction is lower than 5 wt%.

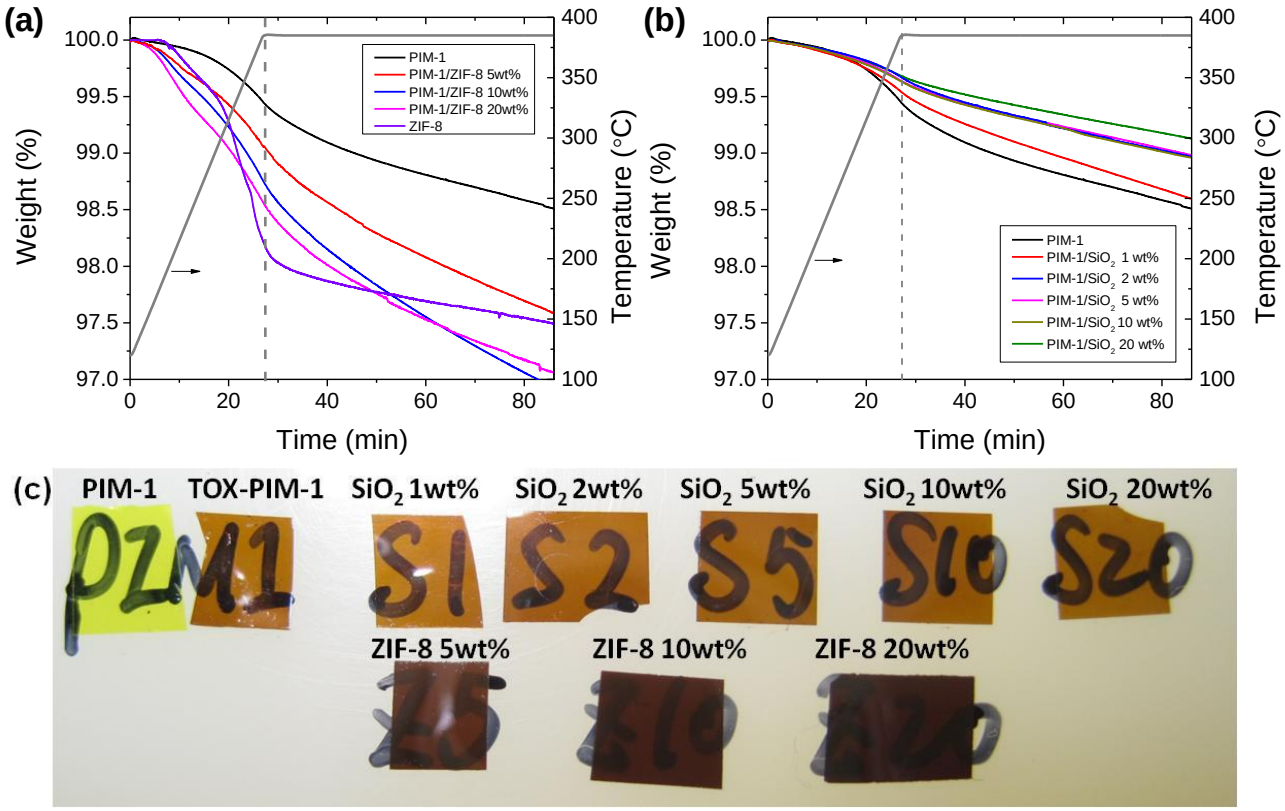

Fig. S9. Thermal oxidative pyrolysis of polymer films. (**a**), PIM-1/ZIF-8 nanocomposite membranes, pure PIM-1 and ZIF-8 are included. (**b**) PIM-1/SiO_2 nanocomposite membranes. (c) Photos of membranes after thermal-oxidative degradation/crosslinking. The samples were purged at 120 ℃ for 1 h under 200 ppm O_2 in argon, then heated to 385 ℃ at 10 ℃/min, then maintained at 385 ℃ for 60 min. Note that the degree of oxidation/crosslinking is lower than those films treated in vacuum oven for gas permeation tests.

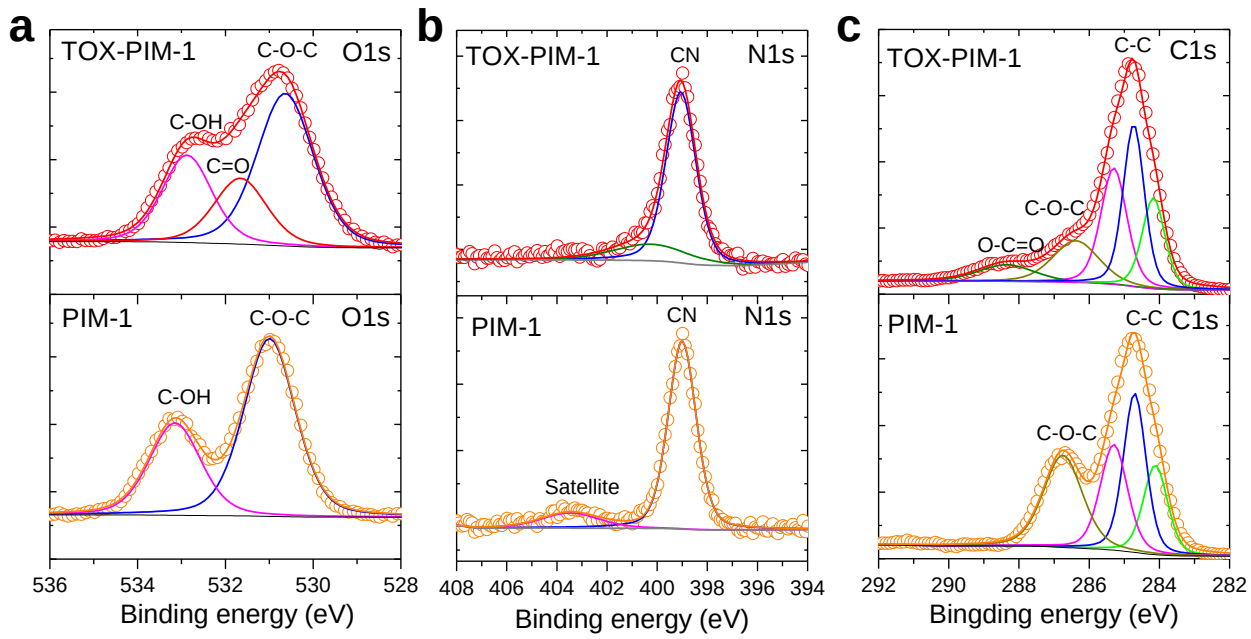

Fig. S10. Probing the chemical bonding. (**a-c**) X-ray photoemission spectroscopy (XPS) spectra of PIM-1 and TOX-PIM-1 polymer films. (**a**) O1s, (**b**) N1s, and (**c**) C1s. Circles: raw spectrum. Lines: deconvoluted peaks, backgrounds, and sum. The PIM-1 film was annealed at 120 ℃ for 24 h. The TOX-PIM-1 film was prepared by heating at 385 ℃ under continuous vacuum (1 mbar) for 24 h. The major difference in O1s spectra is the observation of a higher shoulder peak at binding energies of 531.68 eV, associated with the O-C=O bonds. In the C1s spectra, the peak of C-O-C bonds (ether linkages) at the binding energy of 286.68 eV became relatively weaker in the TOX-PIM-1 film, in comparison to the corresponding peak in original PIM-1 polymer. Chemical bonds corresponding to aldehyde or ketone group (–C=O) in the range of binding energies of 287-288 eV may also exist, but it is difficult to deconvolute them. A new broad weak peak at 288.78 eV, corresponding to O-C=O bond (e.g. carboxylic acid), is observed in the TOX-PIM-1 film. The primary peaks at binding energy of 284.8 eV, corresponding to the overlap of C-C, C-H and C≡N bonds, do not show significant difference in both PIM-1 and TOX-PIM-1 films. As for the N1s spectra of the polymer films, the primary symmetric peak at binding energy of 399.0 eV is attributed to the aromatic nitrile (C≡N) bonds[4]. The peak became asymmetric in the TOX-PIM-1 film, and deconvolution of the peak gives a broad weak peak at binding energy of 400.4 eV, which we can not assign accurately to specific carbon-nitrogen bonds (e.g. C=N) because NO bonds is also possible owing to the oxidation of nitrile groups[4].

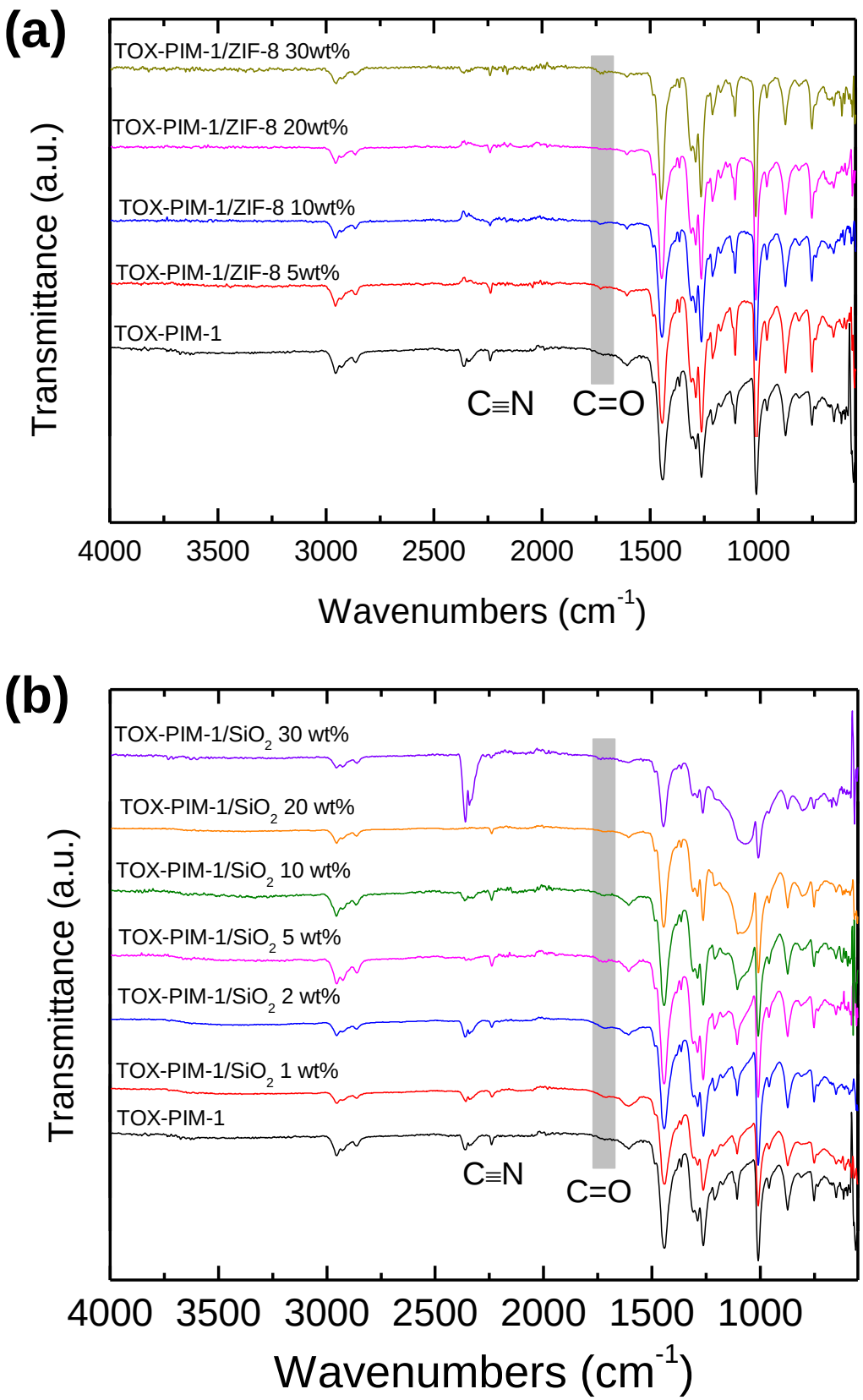

Fig. S11. FTIR spectra of thermal-oxidatively crosslinked PIM-1 polymer composite films.

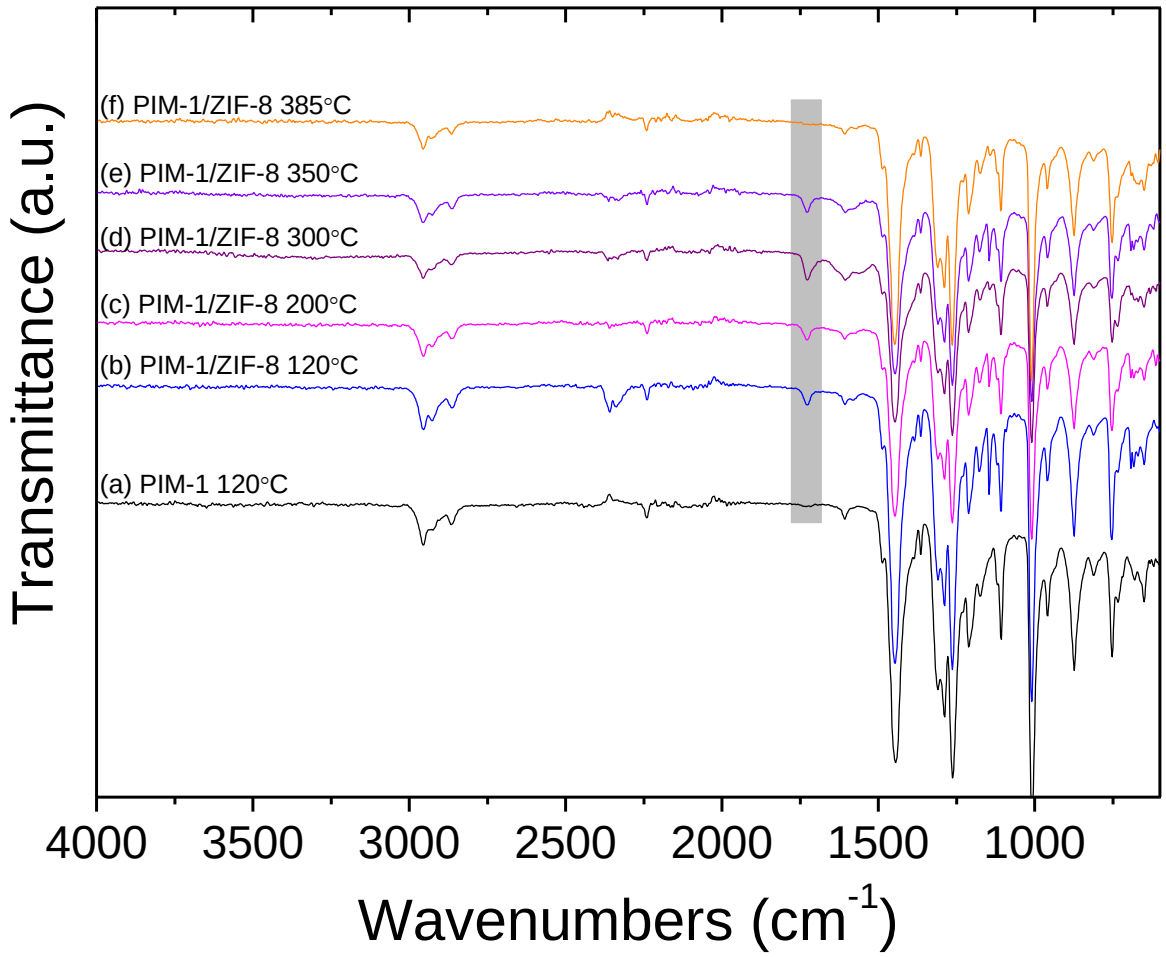

Fig. S12. FTIR spectra of PIM-1/ZIF-8 composite membranes annealed at different temperatures. ZIF-8 loading in PIM-1/ZIF-8 nanocomposites is 20 wt%.

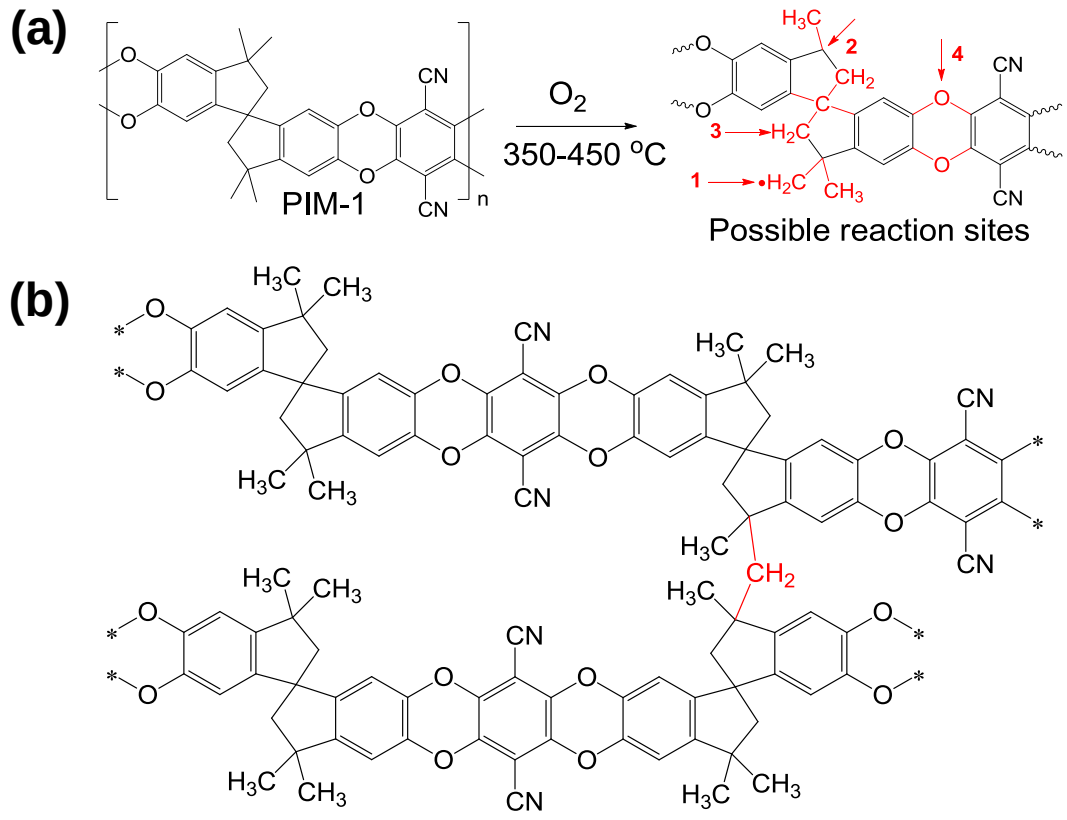

Fig. S13. (a) Possible initial reaction sites of thermal oxidative crosslinking of PIM-1, involving hydrogen abstraction from methyl group, or cleaving of methyl group by oxygen resulting in CO_2 release and a radical site for crosslinking. The thermal crosslinking may also involve intermediate steps such as oxidation and further decarboxylation. Thermal-oxidation is proposed to occur at the large less-selective pores where oxygen molecules diffuse through preferentially. (b) A possible crosslinking pathway through the methyl groups on the spiro-sites. Residual oxidized groups are not shown here. It should be noted that although the oxidative crosslinking mechanism is still not clear, it would not significantly alter the novelty of using the technique to crosslink the polymer nanocomposite membranes incorporated with nanofillers to achieve enhanced diffusion.

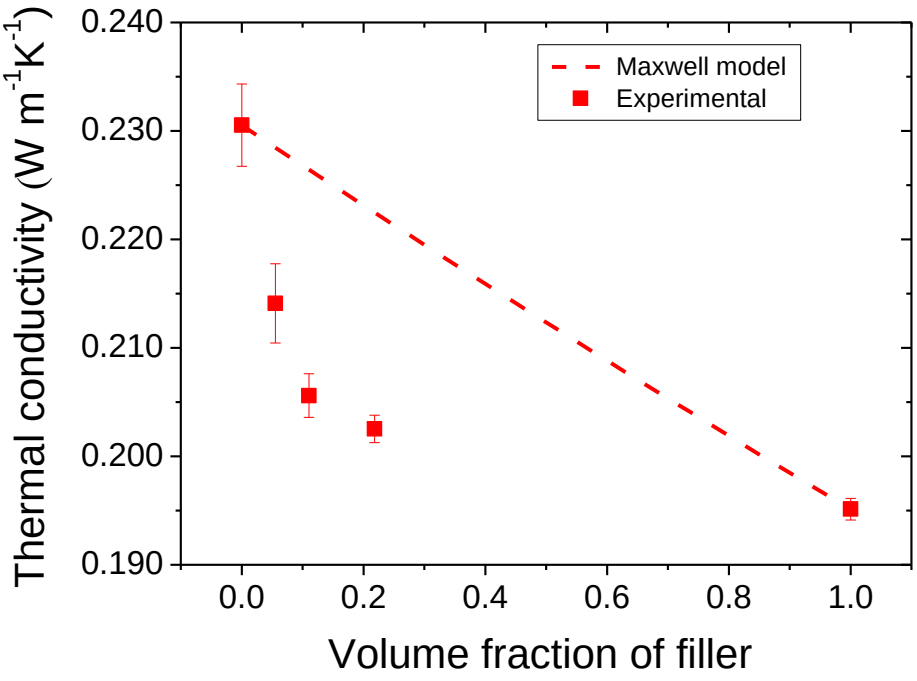

Fig. S14. Thermal conductivity. Dense PIM-1 and PIM-1/ZIF-8 nanocomposite membranes with loading of ZIF-8 nanocrystals at 5, 10, and 20 wt%.

The thermal conductivity of PIM-1 polymer is about 0.23 W m^{-1} K^{-1}, which is in the normal range of conventional polymers (0.1-0.3 W m^{-1} K^{-1}). Therefore, the heat transfer properties during thermal treatment of PIM-1 membranes should be similar to that of conventional polymers. The thermal conductivity of ZIF-8 is not known in the literature. Here, ZIF-8 nanocrystals were dried at 120 ℃ under vacuum and pelletized giving an apparent value of 0.19 W m^{-1} K^{-1} at 295 K, which is likely an underestimation of the intrinsic value due to the presence of voids between the crystals. The thermal conductivity of MOF-5 single crystal gives an intrinsic low value of ~0.3 W m^{-1} K^{-1} at 300 K[5].

The Maxwell equation was used to predict the effective thermal conductivity of nanocomposite membranes (k_{eff}) using the as measured apparent data:

$$k_{eff} = k_c \left[\frac{k_d + 2k_c - 2\phi(k_c - k_d)}{k_d + 2k_c + \phi(k_c - k_d)} \right] \quad \text{(S1)}$$

Where k_c and k_d are the thermal conductivity of continuous phase (polymer) and dispersed phase (fillers), respectively. ϕ is the volume fraction of fillers. The experimental thermal conductivity of nanocomposite membranes is lower than the prediction of Maxwell equation, which is due to the presence of voids and cavities at the interface (not considered in the model).

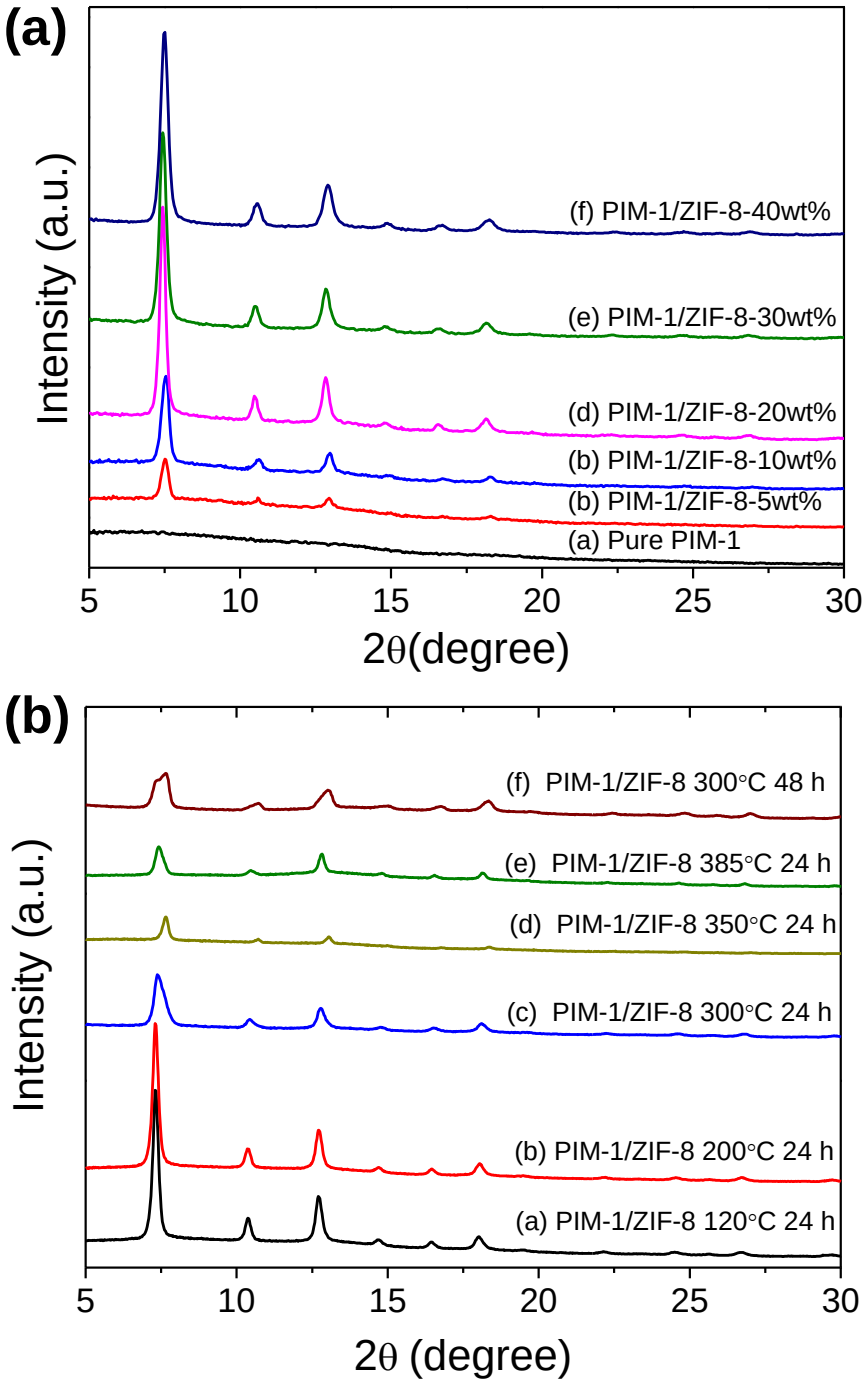

Fig. S15. X-ray diffraction of PIM-1/ZIF-8 membranes. (**A**) PIM-1/ZIF-8 nanocomposite with different loadings of ZIF-8 nanocrystals, samples annealed at 120 ℃ for 24 h; (**B**), PIM-1/ZIF-8 nanocomposite with ZIF-8 loading of 20wt%, thermally treated at different temperatures under vacuum (1 mbar).

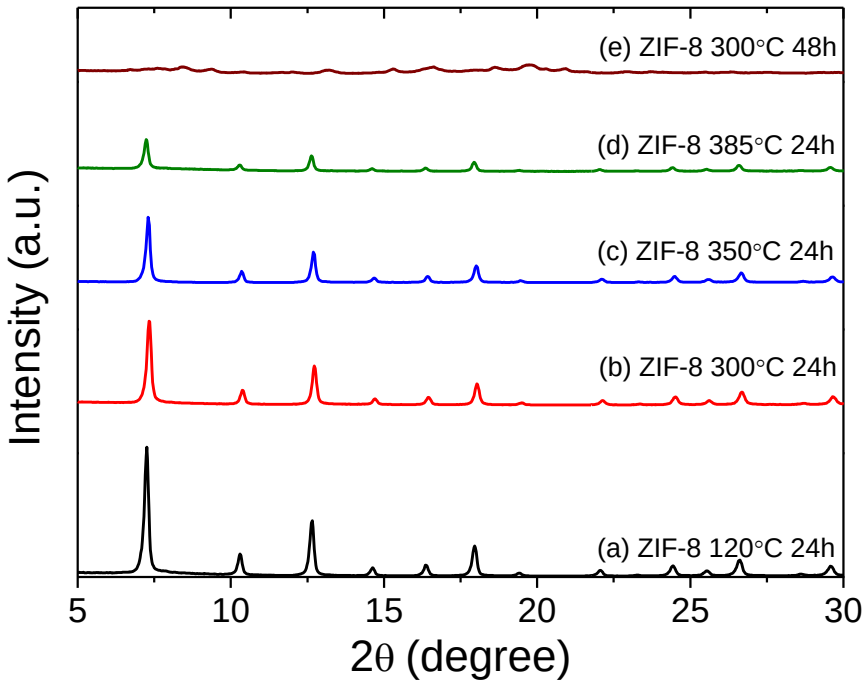

Fig. S16. XRD patterns of ZIF-8 nanoparticles exposed to heat treatment at varied temperatures under vacuum (1 mbar).

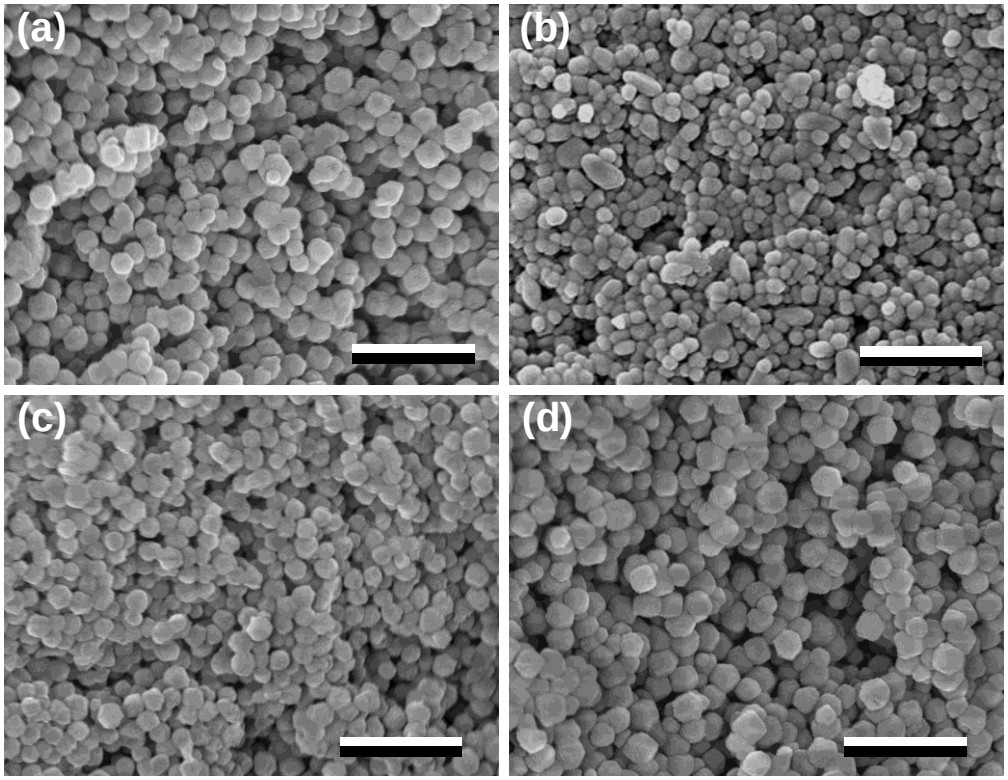

Fig. S17. SEM images of ZIF-8 nanoparticles. (**a**) annealed 300 ℃ for 24 h under vacuum (1 mbar); (**b**) annealed at 300 ℃ for 48 h under vacuum (1 mbar); (**c**) annealed at 350 ℃ for 24 h under vacuum (1 mbar); (**d**) annealed at 385 ℃ for 24 h under vacuum (1 mbar). Scale bar: 500 nm. In extreme instance, the ZIF-8 nanocrystals heated at 300 ℃ for prolonged period of 48 h under vacuum became irregular shaped and lose crystallinity completely.

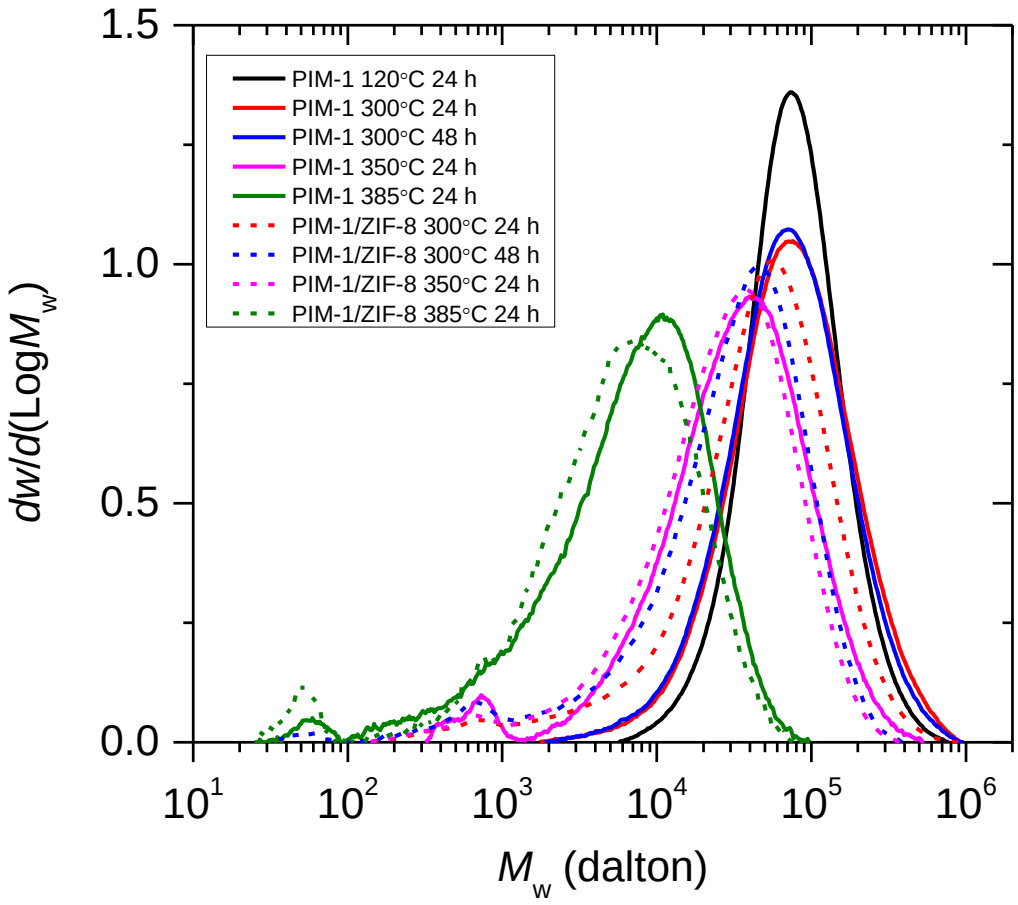

Fig. S18. Molecular weight distribution of the soluble fraction of composite films after thermal treatment at various temperatures. The control PIM-1 polymer films are also included. Nanocomposite membranes containing ZIF-8 heated at intermediate temperature of 300 ℃ for 48 h under vacuum (1 mbar) was still completely soluble in chloroform but lower molecular weight and degradation of ZIF-8 were observed, while pure PIM-1 polymer films heated at 300 ℃ was thermally stable.

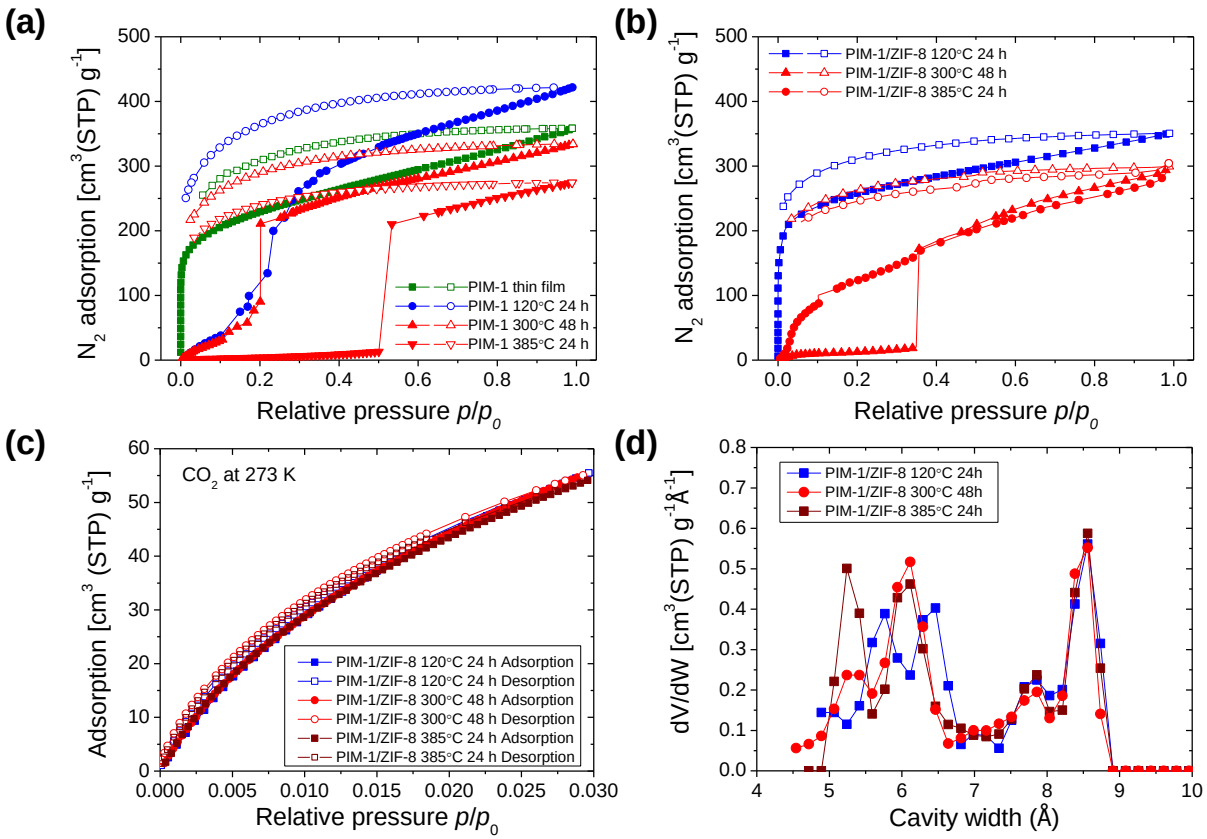

Fig. S19. (a) N_2 adsorption-desorption isotherms of PIM-1 polymer films at 77 K. Squares: PIM-1 thin film (300 nm) dried at 120 ℃ under vacuum; Blue circles: thick dense PIM-1 films (~50 μm) annealed at 120 ℃ under vacuum; Uptriangles: thick dense PIM-1 film annealed at 300 ℃ for 48 h under vacuum. Downtriangles: thick dense PIM-1 film annealed at 385 ℃ for 24 h under vacuum. (**b)** PIM-1/ZIF-8 nanocomposite films. ZIF-8 loading at 20 wt%. Squares: annealed at 120 ℃ for 24 h; Uptriangles: annealed at 300 ℃ for 48 h under vacuum. Circles: crosslinked at 385 ℃ for 24 h under vacuum. **(c)** CO_2 sorption of PIM-1/ZIF-8 nanocomposites treated at various temperatures, and **(d)** derived pore size distribution. All samples were degassed at 120 ℃ under high vacuum prior to gas sorption measurements.

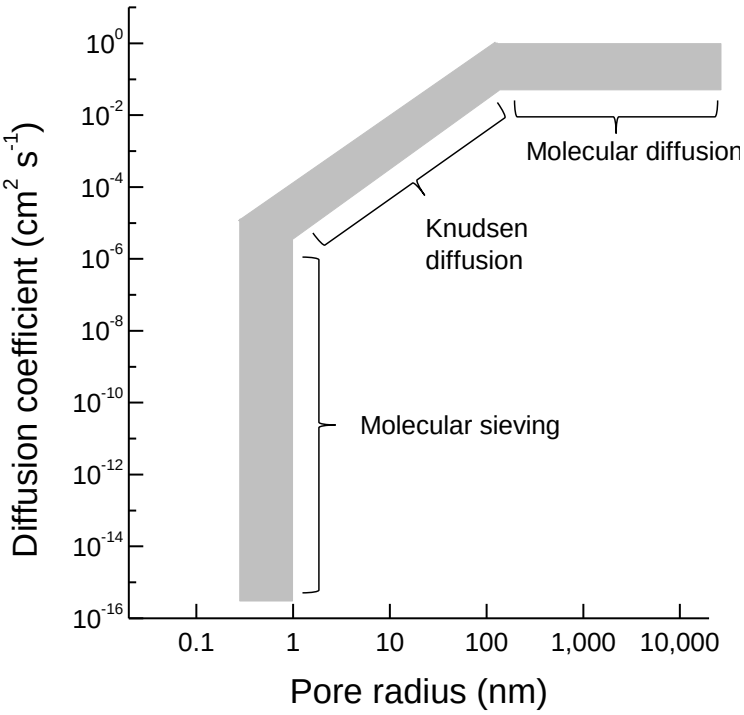

Fig. S20. Influence of pore size on the diffusion coefficient of gas molecules in porous materials. Redrawn from reference.[6]

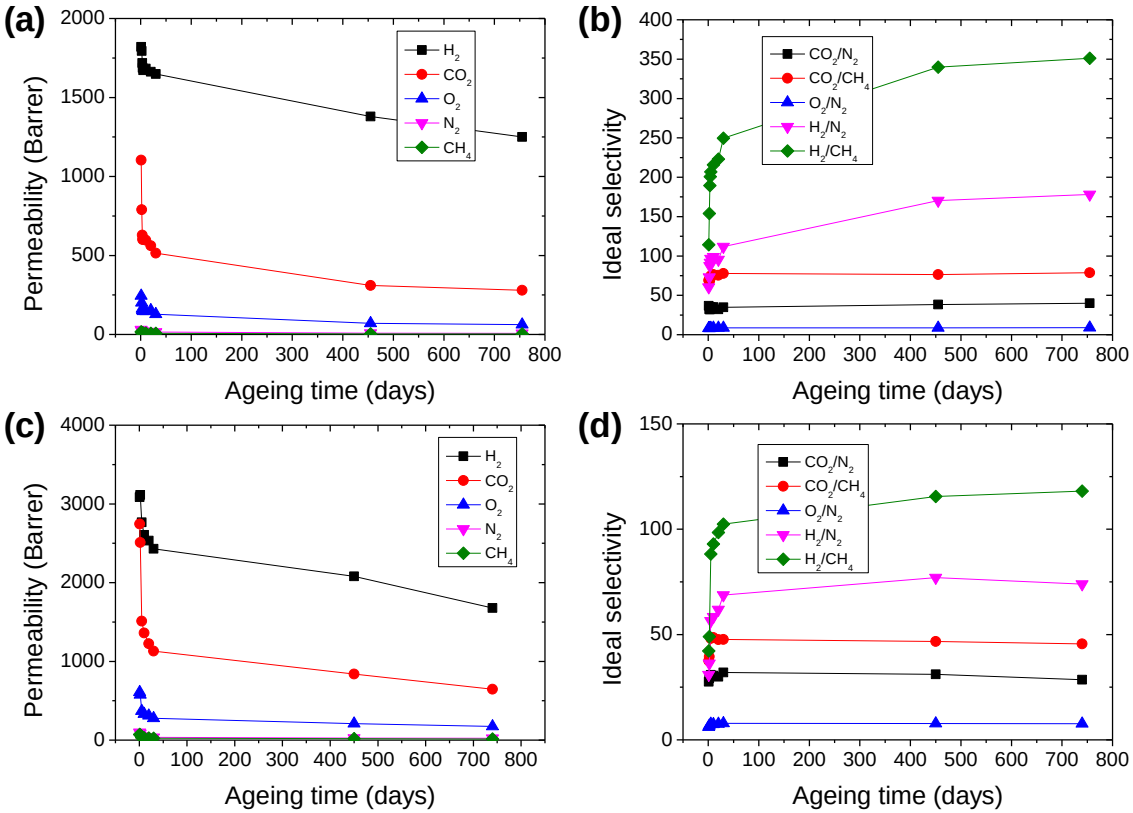

Fig. S21. Gas transport properties of (a-b) TOX-PIM-1 and (c-d) TOX-PIM-1/ZIF-8 nanocomposites (ZIF-8 loading at 5wt%) upon physical aging over two years. These membranes were exposed to vacuum between gas permeation tests. The samples were prepared by thermal oxidative crosslinking at 385 ℃ for 24 h under vacuum (1 mbar).

Table S1. Mechanical properties. The data were derived from stress-strain profiles of PIM-1, thermal oxidatively crosslinked PIM-1 and composite films.

Samples	Tensile strength at break (MPa)	Elongation Strain at break (%)	Young's modulus (GPa)
PIM-1	47.5±2.3	14.3	1.43±0.15
TOX-PIM-1 385°C 1 mbar 24 h	54.8±2.7	4.4	1.72±0.05
TOX-PIM-1/SiO_2 1wt% 385°C 1 mbar 24 h	38	2.4	1.90
TOX-PIM-1/SiO_2 2wt% 385°C 1 mbar 24 h	35	2.3	1.60
TOX-PIM-1/SiO_2 5wt% 385°C 1 mbar 24 h	21	1.4	1.55
TOX-PIM-1/SiO_2 10wt% 385°C 1 mbar 24 h	15	1.0	1.50
TOX-PIM-1/ZIF-8 5wt% 385°C 1 mbar 24 h	23	1.6	1.51
TOX-PIM-1/ZIF-8 10wt% 385°C 1 mbar 24 h	19	1.4	1.39
TOX-PIM-1/ZIF-8 20wt% 385°C 1 mbar 24 h	16	1.3	1.33

Table S2. Young's modulus and Hardness derived from nanoindentation measurement.

Sample	**Young's modulus *E* (GPa)**	**Hardness *H* (MPa)**
PIM-1 120°C 24 h	1.876±0.029	149±4.0
TOX-PIM-1 385°C 1 mbar 24h	1.885±0.039	188±3.0
PIM-1/ZIF-8 20wt% 120°C 24 h	1.954±0.075	159±13.0
TOX-PIM-1/ZIF-8 20wt% 385°C 1 mbar 24h	1.732±0.027	158±4.0

Table S3. Representative gas transport properties of thermally crosslinked PIM polymer nanocomposite membranes. Crosslinked membranes were thermally oxidized at 385°C under vacuum (1 mbar) for 24 h.

Sample	Volume fraction[a]	Permeability (Barrer)					Selectivity				
		H_2	CO_2	O_2	N_2	CH_4	CO_2/N_2	CO_2/CH_4	O_2/N_2	H_2/N_2	H_2/CH_4
PIM-1	0	3361	5040	1020	244	288	20.6	17.5	4.2	13.8	11.7
PIM-1/ZIF-8 5 wt%	0.057	3778	5223	1179	252	309	20.7	16.9	4.7	15.0	12.2
PIM-1/ZIF-8 10 wt%	0.113	5005	5928	1492	282	351	21.0	16.9	5.3	17.7	14.2
PIM-1/ZIF-8 20 wt%	0.223	4977	6342	1521	293	426	21.7	14.9	5.2	17.0	11.7
PIM-1/ZIF-8 30 wt%	0.330	5456	6424	1452	304	370	21.1	17.4	4.8	17.9	14.8
PIM-1/SiO_2 1 wt%	0.005	4068	5381	1116	279	335	19.3	16.1	4.00	14.6	12.1
PIM-1/SiO_2 2 wt%	0.010	4175	5756	1079	282	346	20.4	16.6	3.83	14.8	12.1
PIM-1/SiO_2 5 wt%	0.025	5385	6061	1130	330	427	18.3	14.2	3.42	16.3	12.6
PIM-1/SiO_2 10 wt%	0.051	5614	6193	1229	368	447	16.8	13.9	3.34	15.3	12.6
PIM-1/SiO_2 20 wt%	0.108	5715	7227	1509	453	628	16.0	11.5	3.33	12.6	9.1
PIM-1/SiO_2 30 wt%	0.171	5500	8351	1678	536	754	15.6	11.1	3.13	10.3	7.3
PIM-1/SiO_2 40 wt%	0.243	5544	8505	1734	581	830	14.6	10.2	2.99	9.5	6.7
TOX-PIM-1	0	1820	1104	245	30	16	36.6	69.2	8.1	60.4	114.1
TOX-PIM-1/SiO_2 1 wt%	0.005	1935	1198	266	36	19	33.0	63.5	7.3	53.4	102.6
TOX-PIM-1/SiO_2 2 wt%	0.010	2069	1552	362	49	25	31.7	62.4	7.4	42.2	83.1
TOX-PIM-1/SiO_2 5 wt%	0.025	2405	1824	420	61	33	29.8	55.0	6.9	39.3	72.6
TOX-PIM-1/SiO_2 10 wt%	0.051	2551	2352	492	79	56	29.7	42.3	6.2	32.2	45.9
TOX-PIM-1/SiO_2 20 wt%	0.108	2816	2615	603	101	80	26.0	32.5	6.0	28.0	35.0
TOX-PIM-1/ZIF-8 5 wt%	0.057	3086	2745	608	100	73	27.5	37.6	6.1	31.0	42.2
TOX-PIM-1/ZIF-8 10 wt%	0.113	3230	3199	682	118	104	27.1	30.7	5.8	27.4	31.0
TOX-PIM-1/ZIF-8 20 wt%	0.223	3465	3944	800	139	147	28.3	26.8	5.7	24.9	23.6

[a] Volume fraction of the dispersed in the composites is defined as: $\phi_D=(m_D/\rho_D)/(m_D/\rho_D+m_C/\rho_C)$, where m and ρ refer to the mass and density of the continuous phase (polymer) and dispersed phase (filler).

Table S4. Summary of gas permeability, diffusion coefficient, solubility coefficient, diffusion selectivity and solubility selectivity for thermally crosslinked PIM-1 and nanocomposite membranes.

Samples	P (Barrer)			D (10^{-8} cm^2 s^{-1})			S (10^{-2} cm^3 cm^{-3} $cmHg^{-1}$)			Diffusivity selectivity		Solubility selectivity	
	CO_2	N_2	CH_4	CO_2	N_2	CH_4	CO_2	N_2	CH_4	CO_2/N_2	CO_2/CH_4	CO_2/N_2	CO_2/CH_4
TOX-PIM-1	1104	30	16	23.6	9.2	1.2	49.0	3.8	12.1	2.6	19.2	13.0	4.1
TOX-PIM-1/SiO_2 1 wt%	1198	36	19	24.2	10.7	1.5	49.4	3.4	12.2	2.3	15.7	14.6	4.0
TOX-PIM-1/SiO_2 2 wt%	1552	49	25	30.3	11.4	2.2	51.2	4.3	11.2	2.7	13.6	11.9	4.6
TOX-PIM-1/SiO_2 5 wt%	1824	61	33	39.2	14.7	2.9	46.5	4.2	11.3	2.7	13.3	11.2	4.1
TOX-PIM-1/SiO_2 10 wt%	2352	79	56	47.6	21.8	4.1	49.4	3.6	13.4	2.2	11.5	13.6	3.7
TOX-PIM-1/SiO_2 20 wt%	2615	101	80	53.3	26.7	6.7	49.0	3.8	12.1	2.0	8.0	13.0	4.1
TOX-PIM-1/ZIF-8 5 wt%	2745	100	73	54.5	29.3	5.9	50.3	3.4	12.3	1.9	9.2	14.8	4.1
TOX-PIM-1/ZIF-8 10 wt%	3199	118	104	63.2	37.5	7.5	50.6	3.1	13.9	1.7	8.4	16.1	3.6
TOX-PIM-1/ZIF-8 20 wt%	3944	139	147	83.3	43.9	12.0	47.3	3.2	12.2	1.9	6.9	14.9	3.9

References

1 P. M. Budd, E. S. Elabas, B. S. Ghanem, S. Makhseed, N. B. McKeown, K. J. Msayib, C. E. Tattershall and D. Wang, *Adv. Mater.*, 2004, **16**, 456-459.

2 Q. Song, S. K. Nataraj, M. V. Roussenova, J. C. Tan, D. J. Hughes, W. Li, P. Bourgoin, M. A. Alam, A. K. Cheetham, S. A. Al-Muhtaseb and E. Sivaniah, *Energy Environ. Sci.*, 2012, **5**, 8359-8369.

3 J. Cravillon, S. Münzer, S. J. Lohmeier, A. Feldhoff, K. Huber and M. Wiebcke, *Chem. Mater.*, 2009, **21**, 1410-1412.

4 W. J. Gammon, O. Kraft, A. C. Reilly and B. C. Holloway, *Carbon*, 2003, **41**, 1917-1923.

5 B. L. Huang, Z. Ni, A. Millward, A. J. H. McGaughey, C. Uher, M. Kaviany and O. Yaghi, *Int. J. Heat Mass Transfer*, 2007, **50**, 405-411.

6 M. E. Davis and R. J. Davis., *Fundamentals of Chemical Reaction Engineering*, McGraw-Hill, New York, 2003.